7th International Seminar on
Seismic Isolation, Passive Energy Dissipation and Active Control of Vibrations of Structures
Assisi, Italy, October 2-5, 2001

APPLICATIONS ON SEISMIC ISOLATION AND ENERGY DISSIPATION IN BRIDGES IN CHILE AND VENEZUELA

Mauricio Sarrazin, Maria O. Moroni, Pedro Soto, Rubén Boroschek
Department of Civil Engineering, University of Chile, Santiago, Chile
sarrazin@cec.uchile.cl

Francesco Tomaselli
Senior Design Engineer, Tech. Dept., FIP Industriale (Italy)
tomaselli.fip@fip-group.it

ABSTRACT

A new highway system is being constructed in Chile, including many bridges. Base isolation and passive energy dissipation have been considered in the design of the majority of the large span bridges. Two of those bridges, have been selected for continuous monitoring of earthquake induced vibrations and as prototypes for structural response research. These bridges are the Marga Marga Bridge, base isolated by means of HDRB, and the Amolanas Bridge, which uses a combination of sliding bearing and viscous dampers. This presentation deals with the experience acquired from the instrumentation, records obtained, and analysis of those two bridges.

On the other hand, a description of a special integrated seismic protection-bearing system, at present in phase of installation in the Caracas – Tuy Medio Railway in Venezuela is presented. It comprises bearings equipped with steel dissipating elements that work only during the occurrence of well-determined seismic events. They're produced by FIP Industriale S.p.A (Italy) and are made of special austenitic stainless steel whose mechanical properties are not altered under the effects of heat or temperature variations developed during the dissipation process.

1. CHILEAN BRIDGES: INTRODUCTION

The Marga Marga bridge, located at the city of Viña del Mar, was the first chilean bridge designed considering base isolation with HDRB. This bridge and his instrumentation for continuous monitoring were presented in a previous seminar (Moroni et al, 1999). The analysis of the last important earthquake that struck the bridge and that was registered by the accelerometers' local network is presented in this opportunity.

Another important bridge that has a quite different system for earthquake protection is the Amolanas bridge, in the north – south Pan-American highway. The superstructure of this bridge is supported on sliding bearings, being the longitudinal displacements controlled by means of viscous dampers.

2. AMOLANAS BRIDGE

2.1 Description.

The Amolanas Bridge is located at 309 Km to the North of Santiago, in the North – South Pan-American Highway. It crosses over a very deep, almost dray stream. It consists of a continuous steel box girder 268 m. long, with cantilever structures at both sides. This girder stands on sliding supports in the longitudinal direction, with the exception of the support on the tallest pier, which is fixed in all directions. As it can be seen in figures 1, 2, and 3, there are 3 concrete piers which heights, from South to North, are 22.30, 49.10 and 101.3 m, respectively. Two non-linear viscous dampers are located at each abutment as can be seen in figure 4. The piers are reinforced concrete with octagonal hollowed section, as are shown in figure 5. They stand on individual rectangular foundations supported on rock. These piers as well as the superstructure can be seen in figure 4.

The structural design was done by the Carlos Fernández Casado firm in Spain and the construction by Sacyr Chile.

2.2 Girder supports and dampers

The girder, as it was pointed out before, stands on 10 sliding supports: 2 at each abutment and 2 at each pier. All of them except the two that stands over the third pier from South to North, are free to move only in the longitudinal direction. The structural concept for seismic protection is, in short, as follows.

- In transverse direction, the superstructure is quite rigid as compared with the lateral flexibility of piers. Most of the horizontal seismic forces are therefore transmitted to the abutments. The abutments are anchored to rock and have enough resistance to sustain the bridge structure in that direction. The structure is quite flexible in the transverse direction with a natural period of 1.46 sec, thus the seismic response is substantially reduced.
- In the longitudinal direction the seismic forces are transmitted by the viscous dampers to the abutments, thus dissipating energy in the viscous fluid. The tallest pier, fixed to the superstructure, is supported at the top by it, which transmits the seismic forces to the abutments. The other two piers have an interaction with the superstructure through friction forces between teflon pads and stainless steel plates.

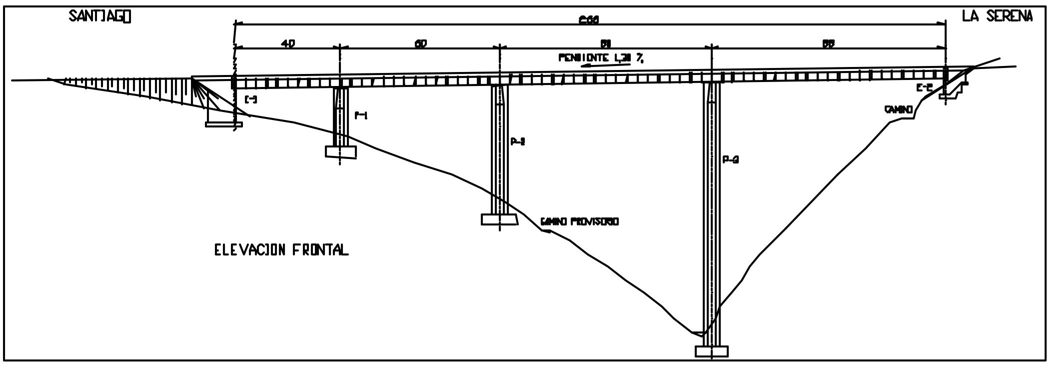

Figure 1. General view, Amolanas Bridge

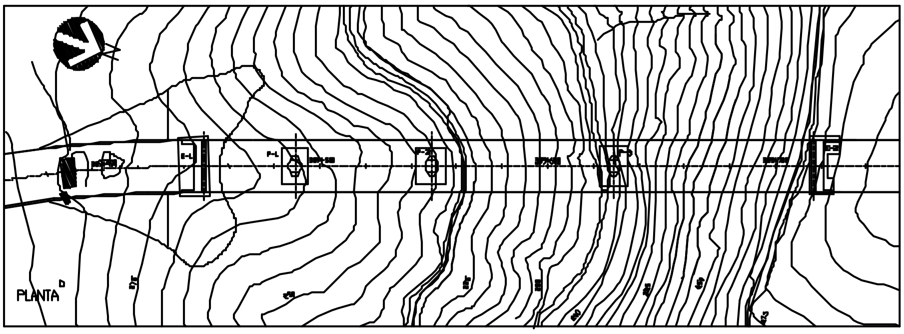

Figure 2. Plan view, Amolanas Bridge

Figure 3. Panoramic view, Amolanas Bridge.

Figure 4. Dampers

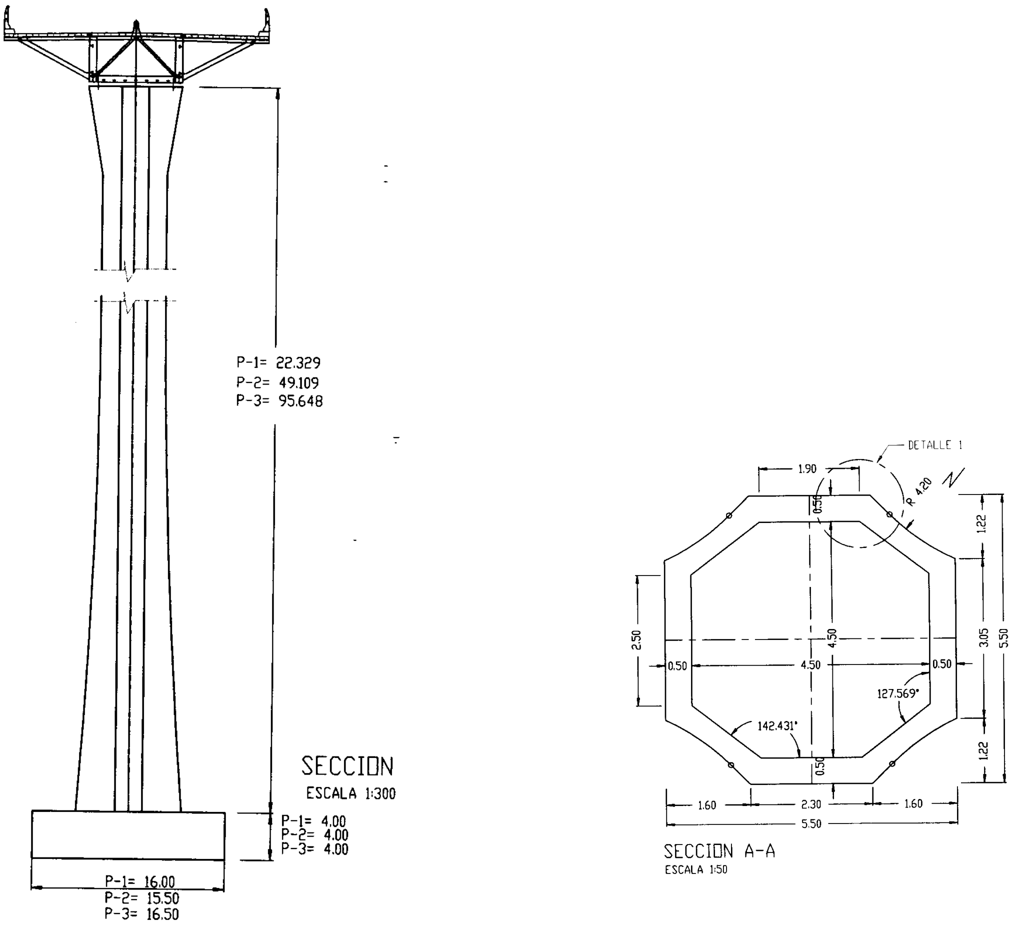

Figure 5. Pier elevation and typical cross section.

The viscous dampers are highly non-linear, having the following characteristic law.

$$F = 3000\ V^{1.5} \pm 15\%$$

Where:

F =	transmitted force [kN]
V =	velocity [m/s]

Thus, forces are very small for low velocities and are almost constant for large velocities. This gives the possibility of thermal expansions with almost no forces and can stand a force up to 3000 [kN] for large velocities.

2.3 Earthquake load. Design Response Spectra and Synthetic Time History Records

In order to determine the design response spectra for the site, as well as a suitable set of time history records, a seismic risk analysis of that location was done. The historic earthquakes of a seismogenetic zone 500 km in diameter were collected and analyzed. It were also determined the possible seismic sources and their characteristic. It was concluded that the earthquake that controls the design is one of M = 8.5 with an epicenter located 30 km off shore at 20 km under the sea. The topography as well as the type of soil were also considered for the definition of the design spectrum and the generation of the synthetic design earthquake records. The design response spectrum is in figure 6.

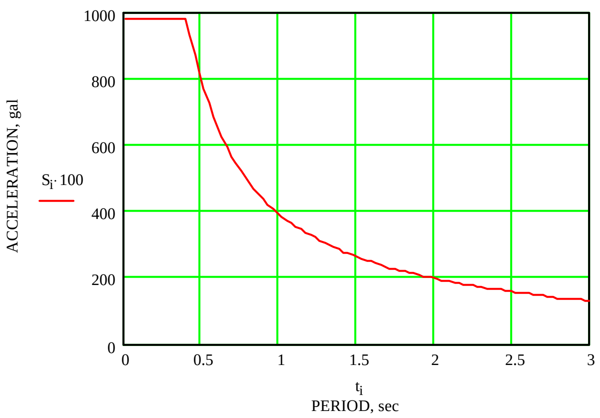

Figure 6. Design response spectrum for R = 1

2.4 Field microvibrations test

In order to get the actual dynamic characteristic of the bridge, a field test was developed, collecting micro-vibration records at different positions and directions on the superstructure of the bridge. Two types of sensors were used for that purpose: three force balance accelerometers (FBA-11 Kinemetric) and six velocity seismometers (Ranger SS-1).

Figure 7. Field microvibrations test.

The aim of this campaign was to obtain the natural frequencies, the modes of vibration, and the damping of the structure. During the recording process the bridge was subjected to traffic; therefore the instruments had to be located at the sidewalks. Figure 7 shows an aspect of the fieldwork.

Given that the response characteristic of each seismometer was different, the output signals had to be normalized to one of them as reference. Considering a seismometer as a 1 DOF system with parameters f_n = natural frequency, ξ = damping ratio, and G = generation constant (the velocity signal is equal to G times the relative velocity of the instrument), the signal $Y_i(f)$ recorded by instrument i would had been $Y_o(f)$ for the reference instrument o. Then the normalized frequency response is:

$$Y_o(f) = \frac{H_0(G_0, f_{n0}, \xi_0, f)}{H_i(G_i, f_{ni}, \xi_i, f)} Y_i(f)$$

where:

$$H(G, f_n, \xi, f) = \frac{4\pi^2 G^2 f^6}{(f_n^2 - f^2)^2 + (2\xi f_n f)^2}$$

A very good fitting between the responses of the 6 instruments standing in parallel at the same position was obtained (Gárate, 2001).

Once the records were corrected, the natural frequencies of vibrations were obtained by means of the power spectral density (Figure 8) and the correlation functions between the different records (Figure 9). The frequencies of vibration obtained are in tables 1 and 2.

.

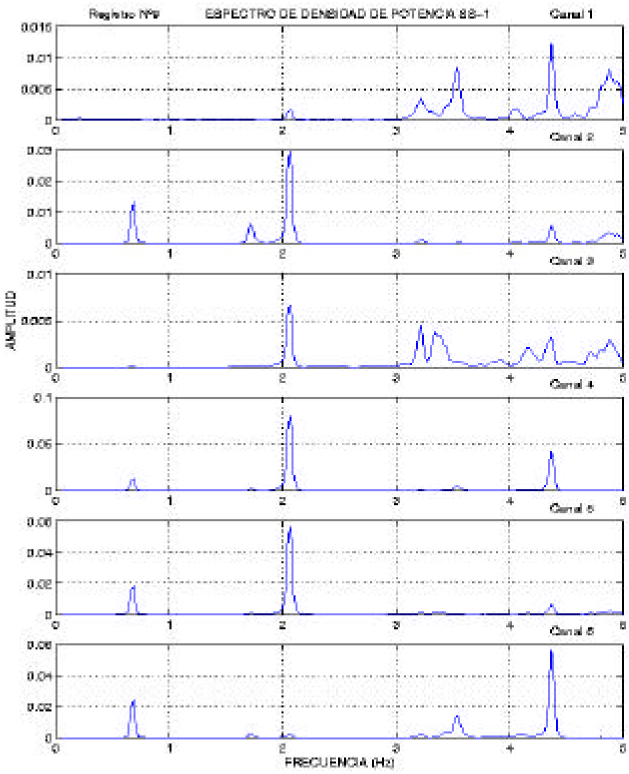

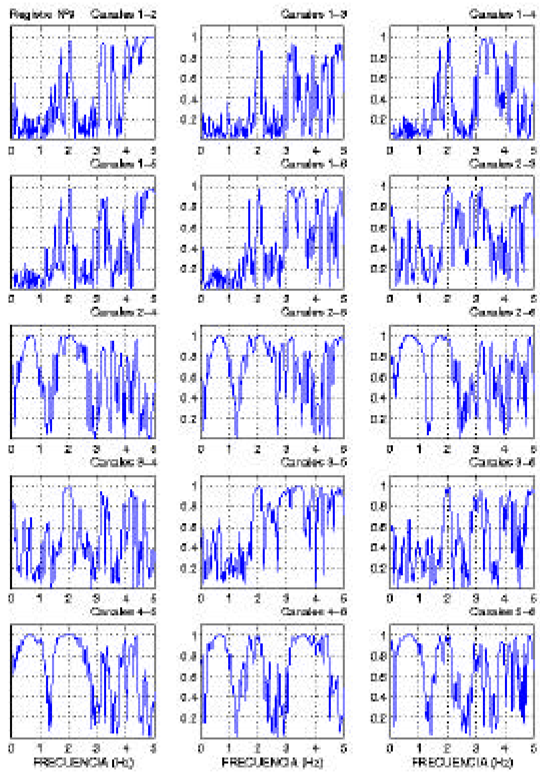

Figure 8. Power Spectral Density, position 9.

Figure 9. Cross Correlations

Mode	Frequency	Period	Damping	Direction
	[Hz]	**[sec]**	**[%]**	
1	0.6834	1.4633	4.40	Transversal -Vertical
2	1.3180	0.7587	1.60	Longitudinal - Vertical
3	1.6598	0.6025	1.64	Transversal
4	2.0503	0.4877	1.21	Transversal –Vertical -Longitudinal
5	2.9534	0.3386	1.01	Longitudinal
6	3.1731	0.3151	0.86	Transversal -Vertical
7	3.3439	0.2991	1.17	Transversal -Vertical -Longitudinal
8	3.5148	0.2845	0.91	Transversal -Vertical
9	4.3691	0.2289	0.64	Transversal -Vertical -Longitudinal

Table 1 : Results obtained with accelerometers FBA-11

Mode	Frequency	Period	Damping	Direction
	[Hz]	[sec]	[%]	
1	0.6834	1.4633	3.4	Transversal
2	1.3424	0.7449	1.46	Longitudinal- Vertical
3	1.7086	0.5853	1.61	Transversal
4	2.0503	0.4877	1.36	Transversal-Vertical-Longitudinal
5	2.9534	0.3386	1.03	Longitudinal
6	3.1975	0.3127	1.47	Transversal - Vertical
7	3.3683	0.2969	0.91	Vertical-Longitudinal
8	3.5148	0.2845	1.26	Transversal
9	4.1738	0.2382	0.92	Longitudinal
10	4.3691	0.2289	0.76	Transversal-Vertical-Longitudinal

Table 2: Results obtained with seismometers SS-1

The modes of vibration can also be obtained from the records, but for determining the direction of the amplitude of motion the phase functions need also to be analyzed. The modes of vibration thus obtained were compared to the ones obtained from an analytical finite element model. Figures 10 to 12 show the 3 first modes obtained from the analytical model. Up to ten modes could be identified from the microvibration records, but only the first 3 modes could be compared between the experimental and analytical results. Figure 13 shows the comparison between both results.

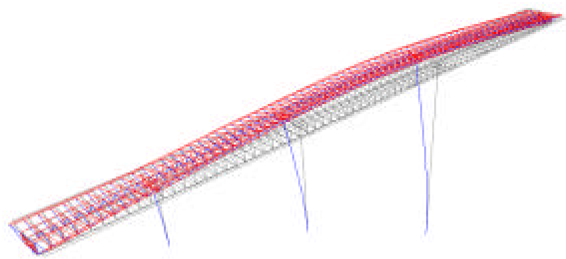

Figure 10. First mode

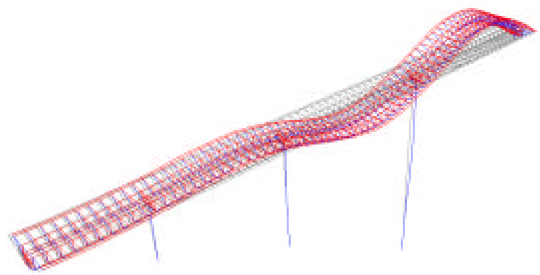

Figure 11. Second mode

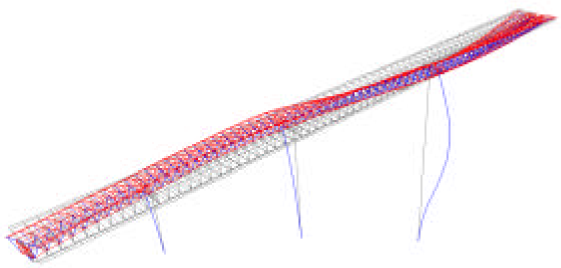

Figure 12. Third mode

2.5 Damping Values

The viscous damping values were obtained by means of the wide band method, that is, by isolating the frequency peak to be studied, then finding the frequencies associated to one half the maximum value and finally obtaining the percentage of critical damping by means of the formula.

$$y = 0.5A(1 - 0.375A^2)$$

where:

$$A = \frac{f_2^2 - f_1^2}{f_2^2 + f_1^2} \qquad , f_1 < f_2$$

With this procedure, the values of table 1 and 2 were determined from the FBA-11 and SS-1 records.

2.6 Discussion on the Amolanas Bridge Investigation

The microvibrations recorded have too low amplitude to produce differential motions at the sliding supports as well as any effect on the viscous dampers. Therefore, a linear elastic model can reproduce the modes of vibration. However, for larger vibrations, as will be the case for the design earthquake, the system will be highly non linear and only a time history analysis would be appropriate. The actual characteristics of the dampers as well as the coefficient of friction of the teflon supports need to be known accurately.

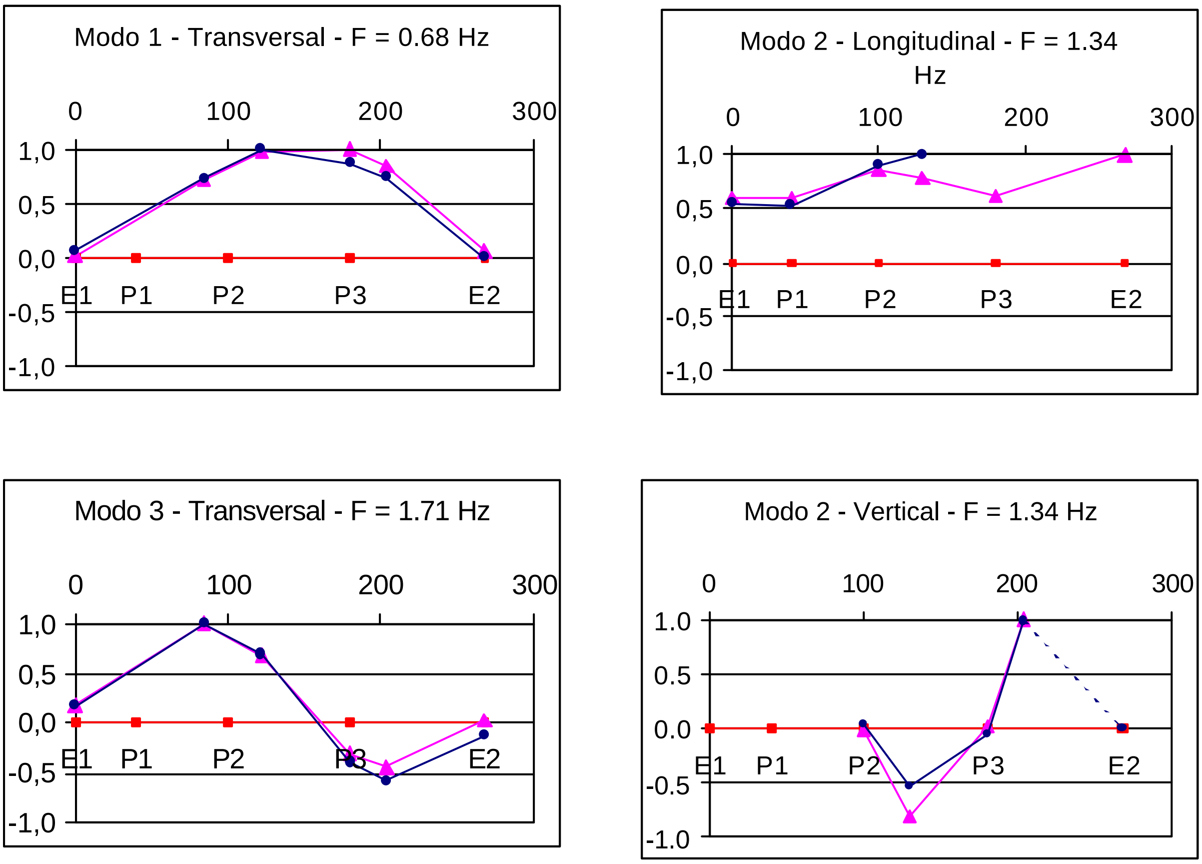

Figure 13. Comparison analytical and experimental modes

2.7 Continuous monitoring

The Amolanas bridge is being instrumented for continuous monitoring of accelerations during earthquake events, (Leiva 2001). The local array of accelerometers will consist of 12 accelerometers, 3 of them on the free field and the rest on the north abutment, on top of piers, and inside the main girder. The information that will be collected from these instruments will be essential for the future development of this kind of structures.

The equipment comprises 12 uniaxial accelerometers type Episensor ES-U of Kinemetric and a K2 controller and data acquisition center. The K2 will be connected by modem to the University of Chile at Santiago. Solar cells will provide the energy for operation. Similar to the systems that are already installed at the Marga Marga bridge and the Metro Viaduct in Santiago, the instruments will start recording whenever any accelerometer reach 0.05 g acceleration. The locations of the different accelerometers are shown in Figure 14.

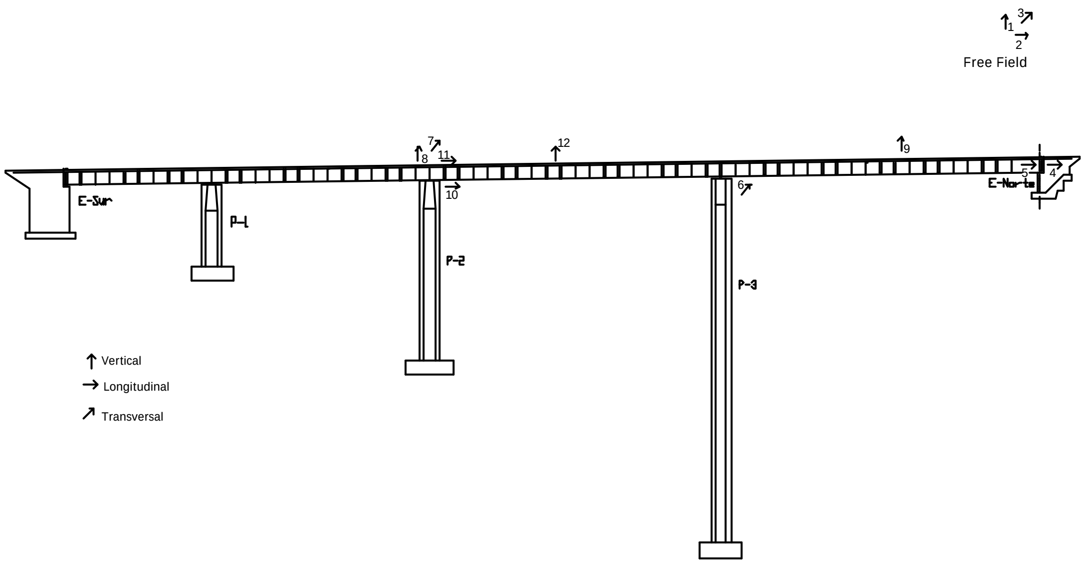

Figure 14. Accelerometers in Amolanas Bridge

3. MARGA MARGA BRIDGE

The Marga Marga bridge has been described previously (Romo, 1999). It is instrumented with a network of 21 accelerometers located at the places that are shown in figure 15. Four sets of records for different events were obtained with these instruments: a) microvibrations produced by traffic during daytime, b) same as a) but at night, c) earthquake of 29/10/98, with a peak acceleration on rock at the site of 0.04g, and d) earthquake of 10/10/98 with peak acceleration on rock of 0.023g. The analysis of those records helped to identify the dynamic characteristics of the bridge. Unfortunate none of those motions was strong enough to produce substantial deformations of the bearings. The maximum bearing deformations at the central pier for the 10/10/98 earthquake were 2.8 mm in the transverse direction and 1.5 mm in the longitudinal one, which represent shear strains of 1.2% and 0.7% respectively, see Figure 16.

For microvibrations, the records obtained at night had less noise than the ones obtained at daytime. All records were used to determine the natural frequencies and modes of vibration.

The records that showed the maximum peak acceleration was the one obtained on the superstructure (slab), in the transverse direction, at the abutments. These accelerations seem to be high frequency vibrations produced by lateral impact between the superstructure and the stoppers. The stoppers are just steel plates sliding against steel plate. There is always a small gap between the plates where clacking occurs.

When the motion in the transverse direction at top of the pier is compared with the one at the superstructure (sensors 6 and 9) acceleration decreasing in the order of 40 to 70% can be seen. The natural frequencies and modes of vibration were determined for the different events using non-parametric methods: PSW, cross correlation's, and filtering. Up to 5 modes of vibrations could be identified, in good agreement between the different events, previous results, and theoretical models.

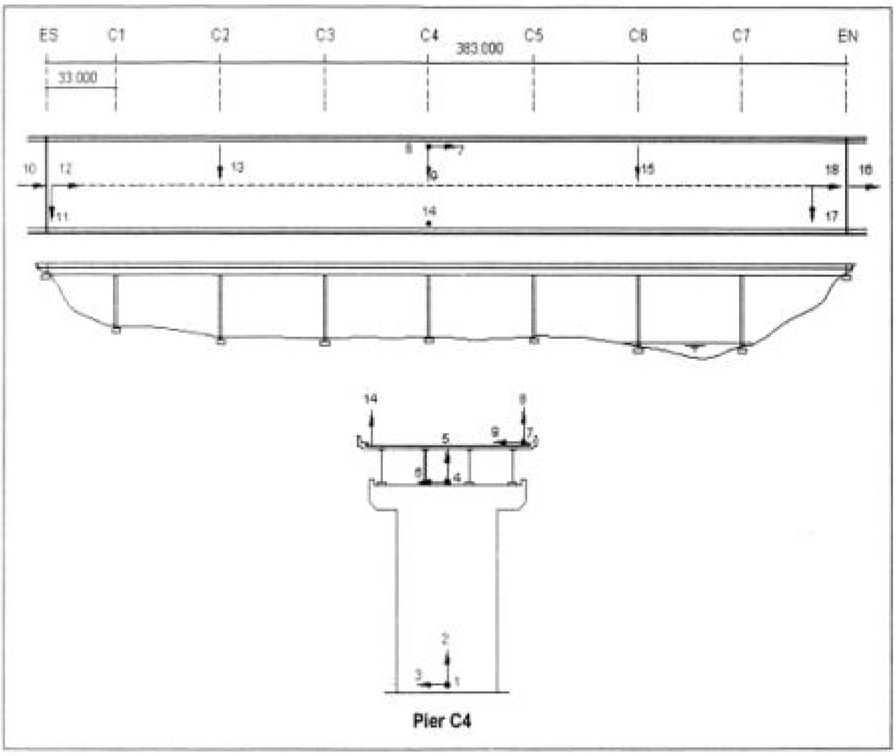

Figure 15. Accelerometers in Marga-Marga Bridge

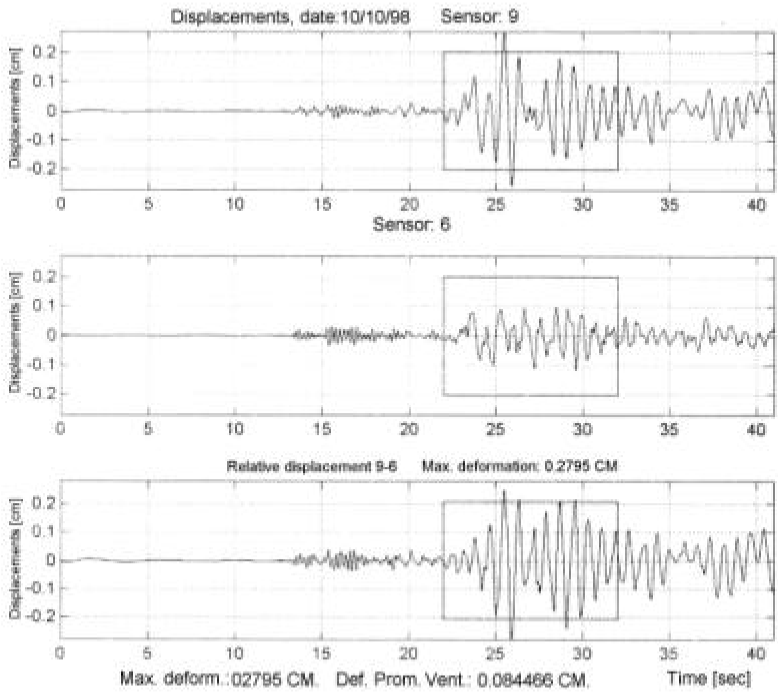

Figure 16. Maximum bearing deformations at the central pier

One objective of this study was to determine the non-linearity of the response with the magnitude of the vibrations. An evidence of this is the differences in the natural frequencies of vibrations obtained from microvibrations as compared with the frequencies obtained from the earthquake records, which are larger. It was verified that even that the earthquake were small, the natural frequencies diminished near 10%. The same was verified by dividing an earthquake record in three parts: before strong motion, the strong motion section and after that. Figure 17 shows the results for sensor 9 (transverse on the slab, at the center of the bridge) for the 29/10/98 earthquake. The Fourier spectrum shows clearly that for the strong motion part of the record the natural frequency is much lower (0.92 Hz as compared with 1.02 Hz).

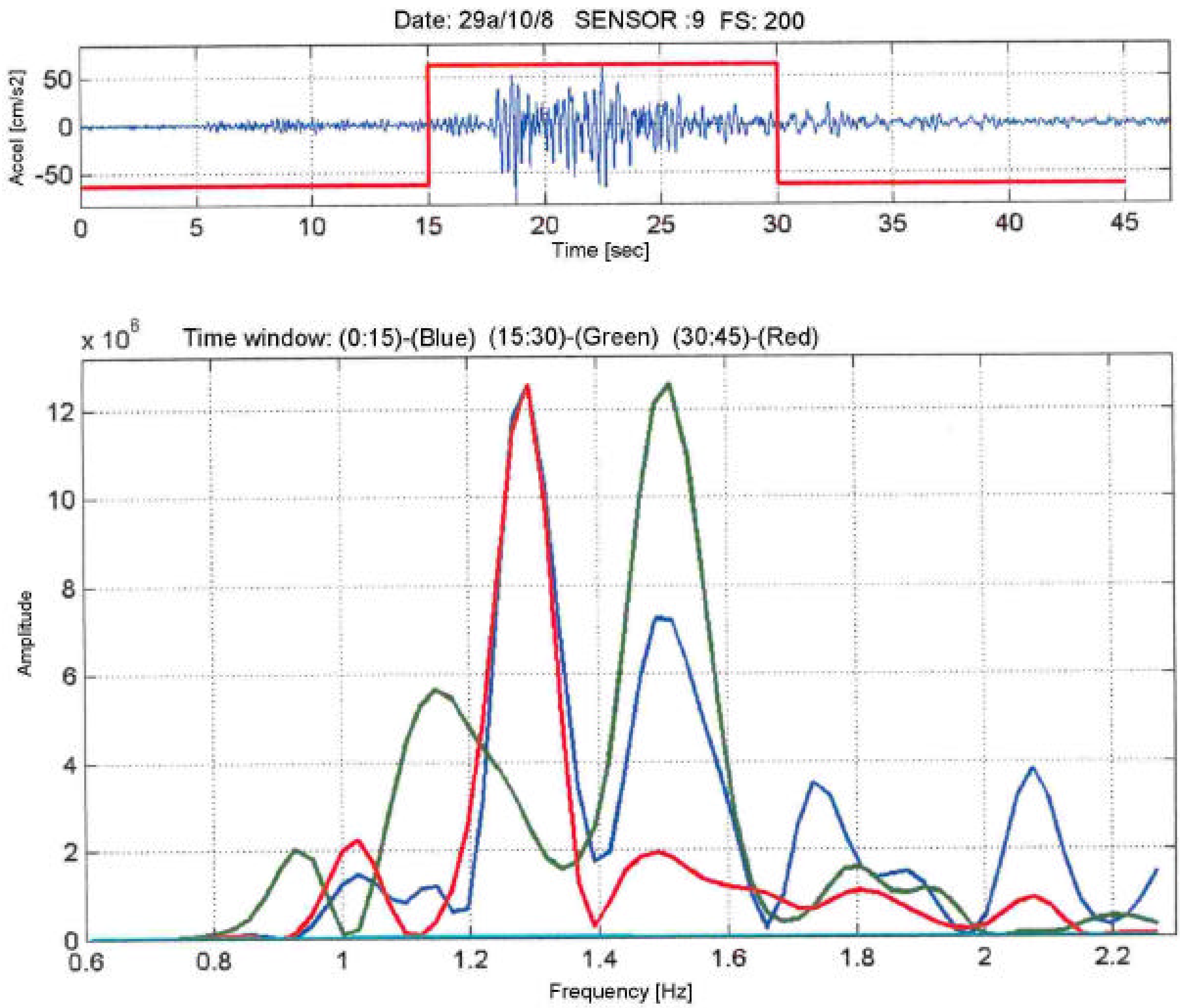

Figure 17. Variations of frequencies during 29/10/98 earthquake

4. VENEZUELAN BRIDGES

Between 1980 and 1990, the government of Venezuela decided to begin construction of a railway system for the central region to link the capital, Caracas, with the port of Puerto Cabello on the Caribbean. This tract represents only a beginning phase of the grandest railway development project in the South American Continent. It’s a continuing alternation of tunnels and viaducts. In particular the project provides for the construction of 8.1 km of viaduct lengths throughout the 40 km extension of railway line.

The railway is located in Venezuela´s north central region, whose seismicity is influenced by the interaction of the Caribbean and South American tectonic Plates. The Seismic Hazard Study (Grases, J., 1993) established a design ground motion with 7.5% probability of exceeding the same during the expected service life (70 years), which is equivalent to an average period return of 900 years. For damage control, the study selected events associated with an average period return of 50 years, which are probably to occur more than once during the service life of the structure.

The study of the bearing + dissipating device system, conducted by the FIP Project Design Department at Selvazzano (in Padova province, Italy), led to the following choices:

Under service conditions the bearings restrain the bridge decks in every direction while allowing thermal and rheological excursions and the rotations produced by elastic deformation through the effects of traffic. For the steel bridge decks, the restraint system is exhibit on the topside of figure 18:

- A fixed bearing + a transverse guided one on the fixed end;
- A longitudinal guided bearing + a free one on the mobile end.

The bearings are provided with sacrificial steel elements (fuses) that during normal service and up to a pre-determined value of horizontal loads impede displacements in desired directions.

Under seismic conditions, when the threshold limit imposed for horizontal loads is exceeded, the fuses shear off and thus do not constitute a restraint to displacements in the directions previously blocked. Thus, the hysteretic steel elements are activated to dissipate seismic energy by opposing displacement and serve to control bridge deck movement. (see bottom side of figure 18).

The devices manufactured (Figures 19) comprise the following main components:

- Vasoflon® pot bearing
- Sacrificial elements (fuses)
- Dissipating hysteretic steel elements (pins)

In this context the description will concentrate on its special components only.

Sacrificial shear elements

Under service conditions, the bearings work elastically owing to the adoption of special connective elements capable of transmitting each horizontal action to the understructure (figure 20). Said elements are self-shearing fuses that work elastically until the breakpoint threshold is reached. When the former shear, the fixed and guided bearings become free, keeping the bridge deck restrained through the dissipating elements incorporated within the bearings themselves.

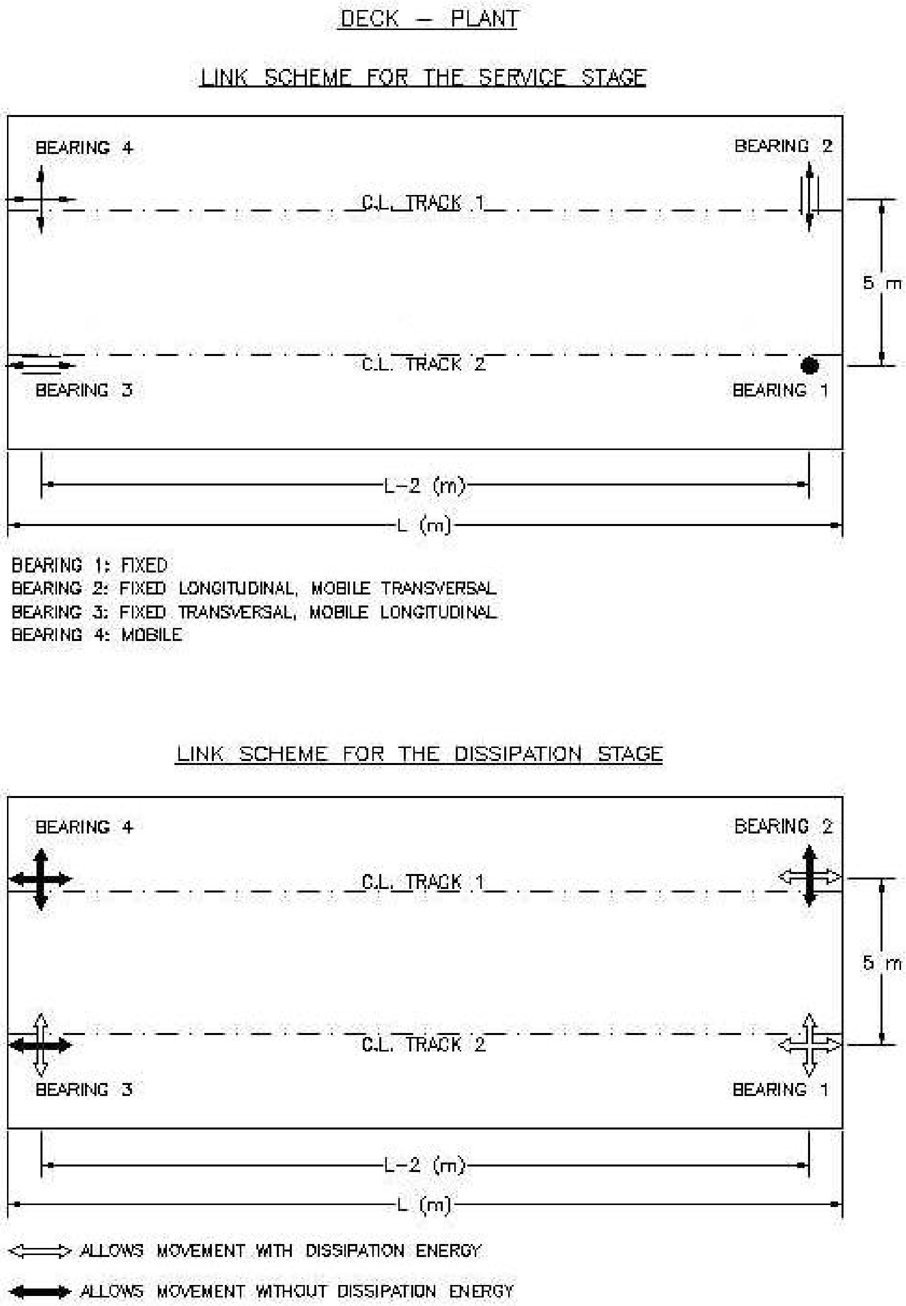

Figure 18. Devices lay-out

Figure 19. Devices in workshop

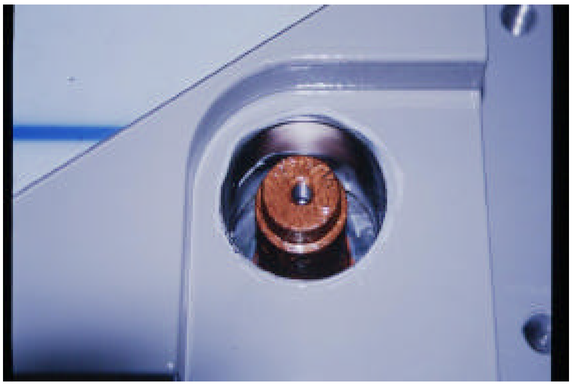

Figure 20. Sacrificial element in the bearing device

Pin Dissipating Elements

The use of axially symmetric dissipating pins together with the special restraint system planned offer practically uniform seismic protection to the structure as well as independent from seismic direction. The adoption of axially symmetric dissipating pin elements guarantees characteristics of multidirectionality and function isotropy.

The hysteretic devices adopted exhibit a behavior that can be represented by a bilinear curve comprising an elastic as well as a plastic branch characterized, given equal deformation, by an increment in load that is decisively reduced. During the seismic event, the dissipating elements follow complete hysteretic cycles with a determined amount of work and dissipating a determined amount of seismic energy, equal to the area of each cycle multiplied by the number of cycles undergone.

The capability of the device to return the bridge deck to a position close to its initial position after a seismic event is practically due to the elastic component within the limits of which the "tail" of the earthquake operates.

The device performance η is nearly 60%, which leads to an equivalent viscous damping equal to 40% ($2\eta/\pi$). To achieve such performance, the dissipating devices are manufactured using special austenitic steels with high physical-chemical characteristics, inalterable in time and capable of resisting a great number of cycles at maximum amplitude, much higher than the number of cycles provided for in the project design.

The properties of the dissipation elements used in the design are determined by individual tests of cyclic reversible loads for a constant amplitude displacement (figure 21 on the left). The number of the cycles that produces the failure occurs, when the specimen is subjected to constant amplitude reversal cycles equal to the selected design maximum displacement, indicates that its service life can be over 20 cycles (graph figure 21 on the right).

Besides these usual tests, separately conducted on the dissipators and the fuses at the FIP Industriale laboratory, additional shaking-table dynamic testing (1:1 scale) on the dissipator-fuse ensemble was undertaken at the ISMES Laboratories in Bergamo (Italy).

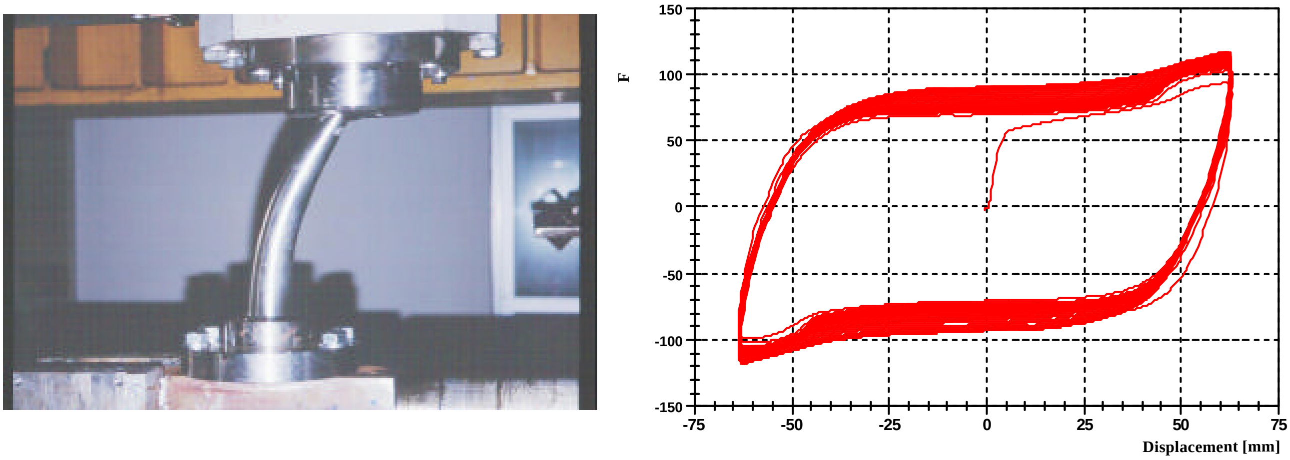

Figure 21. Force – Displacement pin test and experimental curve

5. CONCLUSION

The application of base isolation and passive energy dissipation technology to some new bridges in Chile and Venezuela has been presented. In the case of Chile, two main bridges of different characteristics were analyzed. The Marga Marga bridge is a continuous steel girder bridge supported on HDRB isolators, whereas the Amolanas bridge is also a continuous steel girder bridge but is supported on sliding, stainless steel - teflon bearings and has viscous dampers at the ends extending between the superstructure and the abutments. Both bridges have been instrumented and experimental results are presented in this paper. At the same time theoretical computer model were developed aimed to reproduce the actual motions. Only relative small accelerations were registered because no large earthquakes have occurred. For the Marga Marga bridge, the largest earthquake recorded had a peak ground acceleration on rock of 0.04g, whereas for the Amolanas bridge only ambient vibrations have been registered.

The conclusions coming up from comparison between experimental and theoretical data are that the latter can represent quite well the recorded data. Up to 5 modes of vibrations could be identified from the experimental data. However this is true only for small vibrations where the non-linear effects are absent. The Marga Marga bridge is continuously monitored whereas at the Amolanas bridge a network of 12 accelerometers is being set up in the next months. In the next future, stronger earthquakes will be recorded, which will provide information for further development of these new ways of earthquake protection for bridges.

The earthquakes recorded at the Marga Marga bridge showed the effect of isolation between the upper end of the piers and the superstructure with an important reduction in the horizontal motion, whereas an amplification phenomenon is observed for the vertical component. This phenomenon has also been observed in other isolated structures in Chile.

In the case of Venezuela, a special integrated seismic protection-bearing system, at present in phase of installation in the Caracas – Tuy Medio Railway in Venezuela, has been presented. It comprises bearings equipped with steel dissipating elements that work only during the occurrence of well-determined seismic events. They are made of special austenitic stainless steel whose mechanical properties are not altered under the effects of heat or temperature increases developed during the dissipating process.

Acknowledgements

The writers wish to express their appreciation for the financial support from the Universidad de Chile, Ministerio de Obras Públicas (Proyecto de Innovación Tecnológica) and Fondecyt (Project Nº 1011025 and Nº1970732)

REFERENCES

Gárate, D., 2001, "*Análisis de microvibraciones del Puente Amolanas"*, Civil Engineering Thesis, Universidad de Chile.

Grases, J., Malaver, A., Manzanares, J., 1993, "*Estudio de Amenaza Sísmica"*, Coral 83, Consorcio Contuy Medio.

Leiva, S., 2001, "*Instrumentación del Puente Amolanas"*, Civil Engineering Thesis, Universidad de Chile.

Moroni, M., Boroschek, R., Herrera R., Sarrazin, M., 1999, "*Research and applications on base isolation and passive energy dissipation going on in Chile"*, Proc. Post Smirt Seminar, Cheju, Korea.

Perez, R.J., 2000. "*Dimensionamiento apoyo sismoresistente Proyeto Ferroviario Caracas-Valle del Tuy"*, Seminario Internacional Pontificia Universidad Javeriana, Bogotà, Colombia,

PSN Ingeniería S.C., 1996, "*Criterios y Normas de Diseño para los Viaductos de los Tramos 3 y 4"*, Consorcio Contuy Medio.

PSN Ingeniería S.C., 1998, "*Especificaciones Técnicas para las Pruebas de Caracterización de los Aparatos de Apoyo de los Viaductos Tramos 3 y 4 de la Línea Ferroviaria Caracas - Tuy Medio*" Consorcio Contuy Medio.

Romo D., 1999, "*Análisis de registros sísmicos y microambientales en el puente Marga-Marga"*, Civil Engineering Thesis, Universidad de Chile.

Tomaselli, F., 2000, "*Intervencion Sismoresistente Sobre Puentes y Viaductos"*, Seminario Internacional Pontificia Universidad Javeriana, Bogotà, Colombia.